

# 18F-FDG PET/MR imaging of lymphoma nodal target lesions: comparison of PET standardized uptake value (SUV) with MR apparent diffusion coefficient (ADC)

Hanna Bernstine, MD<sup>a,c</sup>, Liran Domachevsky, MD<sup>a</sup>, Meital Nidam, MSc<sup>a</sup>, Natalia Goldberg, MD<sup>a</sup>, Ifat Abadi-Korek, PhD<sup>a</sup>, Ofer Shpilberg, MD<sup>b</sup>, David Groshar, MD<sup>a,c,\*</sup>

## Abstract

To compare positron emission tomography (PET) standardized uptake value (SUV) with magnetic resonance (MR) apparent diffusion coefficient (ADC) of nodal target lesions in patients with <sup>18</sup>F-fluoro-2-deoxyglucose (FDG)-avid lymphomas by simultaneous PET/MR.

Patients with histologically proven Hodgkin and non-Hodgkin lymphoma underwent PET/MR limited field of view of FDG-avid target nodal lesions. For PET images, a region of interest (ROI) was drawn around the target nodal lesion and the SUVmax and SUVmean was measured. For MR ADC measurements a ROI was placed over the target nodal lesion on diffusion-weighted imaging (DWI) and ADCmin and ADCmean (mean ADC) values within the ROI were recorded.

Thirty-nine patients (19 women, 20 men; 13 patients with Hodgkin lymphoma and 26 with non-Hodgkin lymphoma) were included in the analysis. Sixty-six nodal lesions detected by PET/CT (19 PET-negative and 47 PET-positive) were analyzed by PET/MR. PET/MR quantitative assessments showed that ADCmin and ADCmean were accurate for discriminating positive from negative nodal lymphoma, with an AUC of 0.927 and 0.947, respectively. The ROC curve analysis of ADCmean versus SUVmax and SUVmean was not statistically significant (difference=0.044,  $P=.08$  and difference=0.045,  $P=.07$ ; respectively). A substantial inverse association was observed between ADCmean with SUVmean and SUVmax ( $\rho=-0.611$ ;  $-0.607$ ;  $P<.0001$ , respectively). A moderate inverse association was found between ADCmin with SUVmean and SUVmax ( $\rho=-0.529$ ,  $-0.520$ ;  $P<.0001$ , respectively). Interobserver variability of quantitative assessment showed very good agreement for all variables ( $ICC>0.87$ ).

A significant correlation between ADCs and SUVs is found in FDG avid lymphomas. ADCmean is not inferior to PET SUV in discriminating positive and negative nodal lymphomas. Further larger studies are warranted to validate quantitative PET/MR for lymphoma patient management.

**Abbreviations:** ADC = apparent diffusion coefficient, ADCmean = mean ADC, ADCmin = minimal ADC, AUC = area under the curve, CT = computed tomography, CTAC = CT-based attenuation correction, D5PS = Deauville 5-point score, DWI = diffusion-weighted imaging, FDG = <sup>18</sup>F-fluoro-2-deoxyglucose, FOV = field of view, HL = Hodgkin, MDCT = multidetector computerized tomography, MR = magnetic resonance, MRAC = MR attenuation correction, NHL = non-Hodgkin lymphoma, PET = positron emission tomography, ROC = receiver operating characteristic, ROI = region of interest, SUV = standardized uptake value, SUVmax = maximal SUV, SUVmean = mean SUV.

**Keywords:** diffusion-weighted imaging, lymphoma, PET/MR, standardized uptake value

Editor: Katsuya Yoshida.

HB and LD contributed equally to this manuscript.

The authors have no funding and conflicts of interest to disclose.

<sup>a</sup> Department of Nuclear Medicine, <sup>b</sup> Department of Hemato-oncology, Assuta Medical Centers, <sup>c</sup> Sackler School of Medicine, Tel Aviv University, Tel Aviv, Israel.

\* Correspondence: David Groshar, Department of Nuclear Medicine, Assuta Medical Center, 20 Habarzel Street, Tel Aviv 6971028, Israel (e-mail: davidg@assuta.co.il).

Copyright © 2018 the Author(s). Published by Wolters Kluwer Health, Inc. This is an open access article distributed under the terms of the Creative Commons Attribution-Non Commercial-No Derivatives License 4.0 (CCBY-NC-ND), where it is permissible to download and share the work provided it is properly cited. The work cannot be changed in any way or used commercially without permission from the journal.

Medicine (2018) 97:16(e0490)

Received: 9 October 2017 / Received in final form: 23 March 2018 / Accepted: 28 March 2018

<http://dx.doi.org/10.1097/MD.0000000000010490>

## 1. Introduction

Lymphomas are a very common heterogeneous group of lymphoproliferative malignancies largely separated into Hodgkin and non-Hodgkin lymphoma.<sup>[1–4]</sup> Radiolabeled <sup>18</sup>F-fluoro-2-deoxyglucose (FDG) positron emission tomography (PET)/computed tomography (CT) is the current reference standard for assessment of staging and response of nodal aggressive lymphomas in all baseline studies that are FDG avid.<sup>[5–9]</sup> FDG uptake reflects the metabolic activity of the nodal lesion and is mainly used to evaluate tumor aggressiveness in baseline studies, and to assess the response to treatment and prognosis based on interval changes of FDG uptake during, and after, treatment.<sup>[4,10]</sup> FDG uptake can be evaluated either semiquantitatively or qualitatively. Absolute quantitation is cumbersome and is not practical in busy clinics; therefore, increasing numbers of cancer patients are being evaluated by semiquantitative methods using single-metric standardized uptake values (SUVs).<sup>[11]</sup> In qualitative assessment methods, FDG uptake in the tumor is compared to FDG uptake in various tissues.

In clinical practice, qualitative visual assessment is easier to implement. Current guidelines recommended that FDG PET images be interpreted using the Lugano classification that is based on visual assessment—the Deauville 5-point score (D5PS)<sup>[7,12]</sup>—then simplified into active and nonactive lymphoma using FDG hepatic visual uptake as reference (score 1, 2, 3 as PET negative; score 4, 5 as PET positive).<sup>[5,6,8,9]</sup>

Recently, several studies have suggested that diffusion-weighted imaging (DWI) using magnetic resonance (MR) may be useful for staging and restaging of lymphoma patients.<sup>[13–17]</sup> DWI is based on diffusion of water molecules in the tissue and constitutes the basis for the quantitative apparent diffusion coefficient (ADC). ADC represents tissue diffusivity. It is related to the molecular mobility of water molecules and reflects tissue properties such as the size of the extracellular space, viscosity, and cellularity.<sup>[18]</sup>

Although PET and MRI allow the assessment of different tumor characteristics, similarly to PET, DWI can provide visual assessments of lymphoma nodal lesions by discerning different signal attenuation among tissues, and quantitative assessments using data obtained from ADC maps. However, there are conflicting results and a lack of studies demonstrating a clear benefit of DWI for evaluating lymphoma patients.<sup>[1,19–21]</sup> Moreover, currently there are no accepted criteria for MRI evaluation of lymphoma. The purpose of this study was to compare the quantitative SUV and ADC analysis of nodal target lesions by simultaneous PET/MR in patients with FDG-avid lymphomas.

## 2. Material and methods

### 2.1. Patients

This retrospective study of prospectively collected data was approved by the institutional review board and informed written consent was obtained from all patients (Trial number 2015024). Consecutive patients with histologically proven Hodgkin (HL) and non-Hodgkin lymphoma (NHL) that were scheduled for a clinically indicated <sup>18</sup>F-FDG PET/CT study were contacted by the study coordinator. Patients with no other diagnosis of cancer and without MR contraindications, who consented to undergo a PET/MR study on the same day as the PET/CT study were accrued between April 2016 and March 2017.

Patients were included in the analysis if they had FDG-avid nodal lymphoma at baseline before any treatment, a residual PET-negative lymph node or cluster formation or a positive baseline PET with a distinctive mass-like lesion after treatment, and if nodal target lesions were greater than 15 mm in the longest axis, excluding those with an elongated narrow cortex with fat hilum as proposed by Younes et al.<sup>[9]</sup>

### 2.2. PET/CT imaging

PET/CT was performed using an integrated PET/CT scanner (GEMINI TF, Philips Medical Systems, Cleveland, OH). About 60 minutes after intravenous injection of an FDG dose that varied from 370 to 666 MBq according to the patient's weight. Diluted iodinated contrast material (800–1000 mL) was administered orally for bowel opacification. Contrast-enhanced 64-slice multi detector computerized tomography (MDCT) was performed from the skull base to the mid-thigh with a tube voltage of 120 kVp, spiral CT at 0.8 seconds per rotation with modulated 30 to 250 mAs, section thickness of 3.00 mm, and 3.00 mm interval

with image reconstruction every 3.0 mm. All of the patients, excluding those with known iodine hypersensitivity or renal insufficiency, received intravenous iodine contrast media (1.5 cm<sup>3</sup>/kg; Omnipaque 300; iohexol 0.623 g/mL, GE Healthcare Inc. Princeton, NJ). PET emission images were obtained using a weight-based protocol, with 2 minutes of acquisition per bed position with 5 to 6 bed positions from the skull base to the mid-thigh. PET data were reconstructed using three-dimensional ordered subset expectation maximization (3D-OSEM; 3 iteration and 20 subsets) on 144 matrix with CT-based attenuation correction (CTAC).

### 2.3. PET/MR imaging

Following the PET/CT examination, a limited field of view (FOV) simultaneous PET/MR study was performed on the Biograph mMR (Siemens AG, Healthcare Sector, Erlangen, Germany) about 80 to 100 minutes after injection. For each patient, a nuclear medicine physician (D.G., with 13 years of PET/CT experience) chose the FOV with the most FDG-avid target nodal lesion. Nodal target regions included the following: low cervical right and left, axillary right and left, mediastinal, retroperitoneal, mesenteric, pelvic right and left and inguinal right and left; therefore, the limited PET/MR FOVs were either thorax, abdomen, or pelvis.

MR sequences included: coronal Dixon-based sequence for MR attenuation correction (MRAC) followed by coronal T2-weighted half-Fourier acquired single turbo spin echo (HASTE), inversion recovery (IR)-based axial T2-weighted HASTE without and with fat suppression (FS), axial T1-weighted volumetric interpolated breath-hold examination (VIBE) Dixon, and DWI with *b*-values of 50, 200, 600, and 800 sec/mm<sup>2</sup>.

PET data were acquired simultaneously with an acquisition time of 4 minutes in the list mode with the following reconstruction parameters: High-definition PET +ordered subset expectation maximization (OSEM) iterative algorithm, 3 iteration and 21 subsets, Gaussian filter: FWHM 4 mm; relative scattered correction.

### 2.4. PET/MR imaging interpretation

The images were independently analyzed by 2 specialists: a nuclear medicine specialist (H.B., with 10 years of experience in PET/CT and 2 years of experience in PET/MR), and a specialist with dual board certification in radiology and nuclear medicine (L.D., with 6 years of experience in PET/CT and body MR and 2 years of experience in PET/MR). The reviewers were aware that the limited PET/MR studies were obtained from patients with lymphoma who underwent same-day PET/CT, and that the target regions were chosen from the PET/CT study, but were blinded to the PET/CT results and all other clinical information.

Dedicated software (Syngo.via; Siemens Healthcare, Erlangen, Germany) was used for visual assessment of MR DWI images and for PET/MR metrics measurements. The most apparent nodal lesion in each target region was chosen, and up to 3 target nodal lesions from separate regions were selected to limit bias from one single target region in any single patient.

For PET images, SUV calculations normalized for body weight were determined. For lesion measurements, the maximal SUV (SUVmax) and the mean SUV (SUVmean) measured were used. A region of interest (ROI) was drawn around the target nodal lesion and all ROIs were visually evaluated on axial, sagittal, and coronal planes to make certain that the ROI is well located in the desired area.

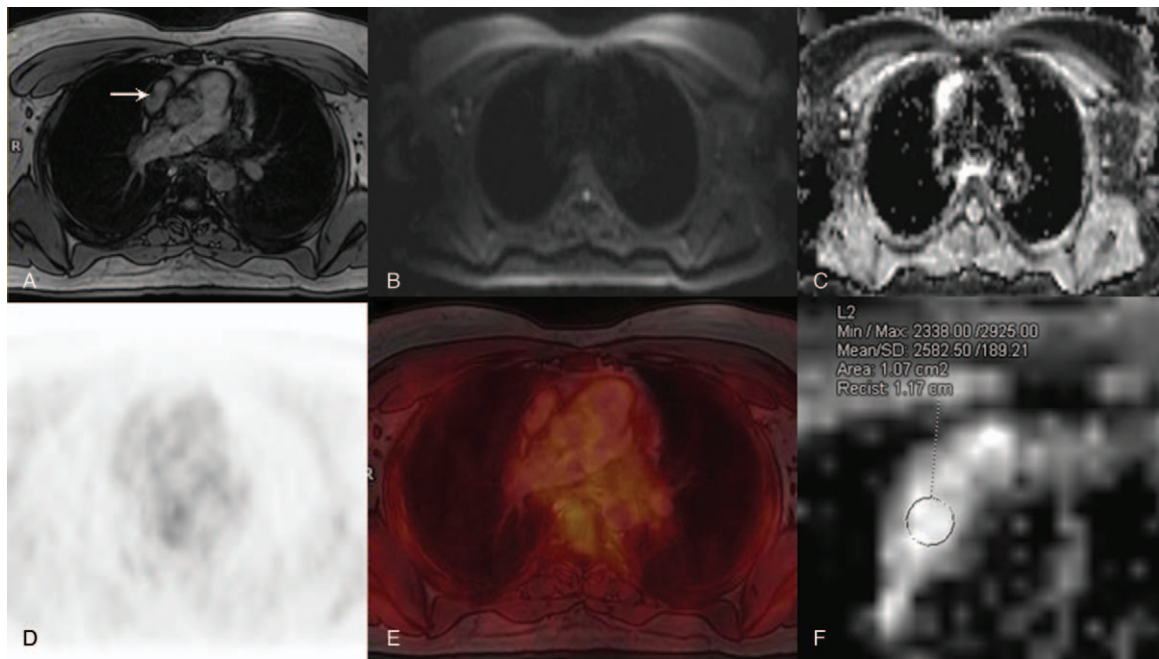


**Figure 1.** 28-year-old man with Hodgkin lymphoma, presented for post treatment evaluation. (A) Axial T1-weighted in-phase image demonstrating residual right upper mediastinal mass (arrow) (B, C). Axial diffusion-weighted ( $b$ -value = 800  $\text{sec}/\text{mm}^2$ ) and ADC images showing no evidence of visual restricted diffusion. (D, E). Axial PET and fused images demonstrating no evidence of FDG uptake. (F). ADC measurements of the mediastinal residual mass with ADCmean of  $2582 \pm 189$ , consistent with no evidence of restricted diffusion. ADC = apparent diffusion coefficient, ADCmean = mean ADC, FDG =  $^{18}\text{F}$ -fluoro-2-deoxyglucose, PET = positron emission tomography.

Quantitative assessment of ADC was performed on the same target lesion chosen for the PET part of the study. For quantitative assessment, a ROI was placed over the target nodal lesion on DWI and the minimal and mean ADC (ADCmin and ADCmean, respectively) values within the ROI were recorded ( $\text{sec}/\text{mm}^2$ ) (Figs. 1 and 2).

### 2.5. Reference standard

PET/CT images were interpreted independently by a nuclear medicine specialist (D.G. with 13 years of experience in PET/CT). The expert reader had access to all available FDG PET/CT and clinical information with a follow-up of at least 6 months to determine PET-positive and PET-negative nodal lymphoma.

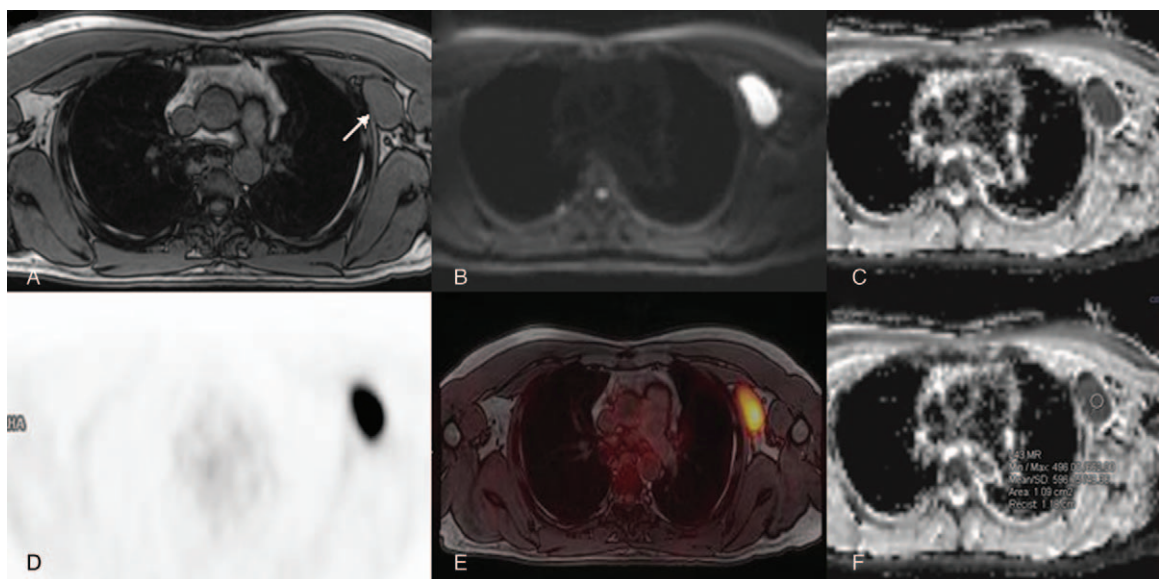


**Figure 2.** 39-year-old man with non-Hodgkin lymphoma, presented for initial staging. (A) Axial T1-weighted in-phase image demonstrating left axillary lymph node (arrow) (B, C). Axial diffusion-weighted ( $b$ -value = 800) and ADC images showing visual restricted diffusion. (D, E). Axial PET and fused images demonstrating intense FDG uptake. (F). ADC measurements of the residual mass with ADCmean of  $597 \pm 48$ , consistent with restricted diffusion. ADC = apparent diffusion coefficient, ADCmean = mean ADC, FDG =  $^{18}\text{F}$ -fluoro-2-deoxyglucose, PET = positron emission tomography.

**Table 1****Patient baseline characteristics.**

Parameter	Patients analyzed n = 39
Gender, n (%)	
Females	19 (48.7%)
Males	20 (51.2%)
Mean age, years (range)	52 (22–81)
Lymphoma type, n (%)	
Hodgkin	13 (33.3%)
Non-Hodgkin	26 (66.6%)
Diffuse large B cell	15 (38.5%)
Follicular	11 (28.2%)
Lesions detected by PET/CT	n (median size; range)
PET-negative	19 (2.9 cm; 1.6–6.5 cm)
PET-positive	47 (2.9 cm; 1.5–8.0 cm)

CT=computed tomography, PET=positron emission tomography,

**Table 2****The median and range of the SUV and ADC variables.**

	PET-positive nodal lesions N = 47	PET-negative nodal lesions N = 19	P value
	Median (range)	Median (range)	
ADCmin, sec/mm <sup>2</sup>	494 (202–2628)	2190 (671–3078)	<.0001
ADCmean, sec/mm <sup>2</sup>	675 (324–2819)	2819 (1119–3558)	<.0001
SUVmean	7.23 (1.55–30.30)	1.26 (0.57–2.14)	<.0001
SUVmax	10.0 (1.9–36.4)	1.4 (0.88–3.84)	<.0001

ADC=apparent diffusion coefficient, ADCmin=minimal ADC, ADCmean=mean ADC, PET=positron emission tomography, SUV=standardized uptake value, SUVmax=maximal SUV, SUVmean=mean SUV.

Target nodal lesions were prospectively interpreted as any lymph node or cluster formation or mass-like lesion by the FDG-PET/CT and was scored according to the visual 5-point scale scoring system (D5PS):<sup>[7,22]</sup> 1 = no uptake; 2 = uptake < mediastinum; 3 = uptake > mediastinum but < liver; 4 = uptake more than liver uptake; 5 = markedly increased uptake at any site and/or new sites of disease.<sup>[5,6,8,9]</sup> D5PS scores of 1–3 were considered as PET-negative and D5PS scores of 4 and 5 were considered as PET-positive for nodal lymphoma and were used as the reference standard for all target nodal lesions as proposed by the International Working Group Consensus Response Evaluation Criteria in Lymphoma (RECL 2017).<sup>[9]</sup>

**2.6. Statistical analysis**

Data are represented by median (range). The Mann–Whitney test was used to compare size, SUVs, and ADCs variables of positive and negative nodal lesions. The Spearman rank correlation coefficient (rho) was used to assess the relationship between SUVs and ADCs. Receiver operating characteristic (ROC) curves were drawn and the area under the curve (AUC) was calculated to evaluate the accuracy of SUVs and ADCs for discriminating positive from negative lymphoma. Pairwise comparisons of ROC curves were obtained.

Absolute ICC was used to assess the degree of interobserver reliability for SUVs and ADCs. A *P* value ≤ .05 was considered statistically significant. All statistical analyses were performed using MedCalc for Windows, version 17.5.5 (MedCalc Software, Ostend, Belgium).

**3. Results**

Sixty patients were accrued into the study between April 2016 and March 2017. Fourteen patients were excluded due to complete response to treatment without a residual nodal target lesion > 1.5 cm in the longest axis, 6 patients had nondiagnostic ADC maps due to artifacts and the FOV of 1 patient was mistakenly scanned without any nodal target lesion. Therefore, 39 patients were included in this analysis. Patient baseline characteristics are shown in Table 1. There were 19 women (mean age 57, range 25–69) and 20 men (mean age 51, range 22–81). Thirteen patients with HL and 26 with NHL (15 diffuse large B-cell and 11 follicular), none had extra-nodal lymphoma lesions.

Sixty-six nodal target lesions detected by PET/CT (19 residual nodal PET-negative [28.8%] and 47 PET-positive lymphomas [71.2%]) were analyzed qualitatively and quantitatively on the simultaneous PET/MR study. There was no significant difference in size between PET-positive (2.9 cm, range 1.5–8.0 cm) with PET-negative (2.9 cm, range 1.6–6.5 cm) (*P* = .45) nodal lesions. Thirty-seven nodal lesions were found in the thorax FOV, 16 in the abdomen FOV and 13 in the pelvis FOV.

**3.1. Quantitative assessment**

Quantitative PET/MR obtained for nodal PET-positive lymphoma were significantly different from the obtained for nodal PET-negative lymphoma (Table 2). A substantial inverse association was observed between ADCmean and SUVmean (rho = −0.611, *P* < .0001) and between ADCmean and SUVmax (rho = −0.607, *P* < .0001) (Fig. 3). A moderate inverse association was found

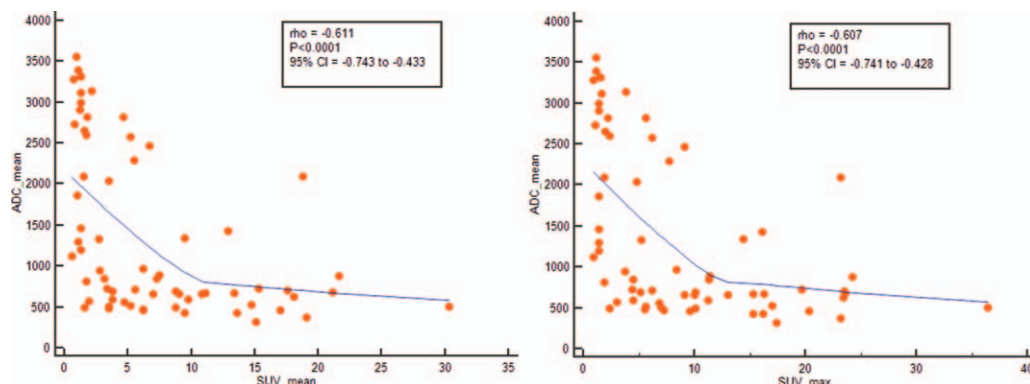


**Figure 3.** Scatter diagram with trend line showing correlation between ADCmean and SUVmean (left) and between ADCmean and SUVmax (right). ADCmean=mean ADC, SUVmean=mean SUV.

**Table 3**  
Correlation between PET/MR metrics SUV and ADC.

Spearman (rho) correlation	SUVmean	SUVmax
ADCmean	-0.61 (-0.74/-0.43) $P < .0001$	-0.61 (-0.74/-0.43) $P < .0001$
ADCmin	-0.53 (-0.68/-0.33) $P < .0001$	-0.52 (-0.68/-0.32) $P < .0001$

ADC = apparent diffusion coefficient, ADCmean = mean ADC, ADCmin = minimal ADC, PET = positron emission tomography, SUV = standardized uptake value, SUVmax = maximal SUV, SUVmean = mean SUV.

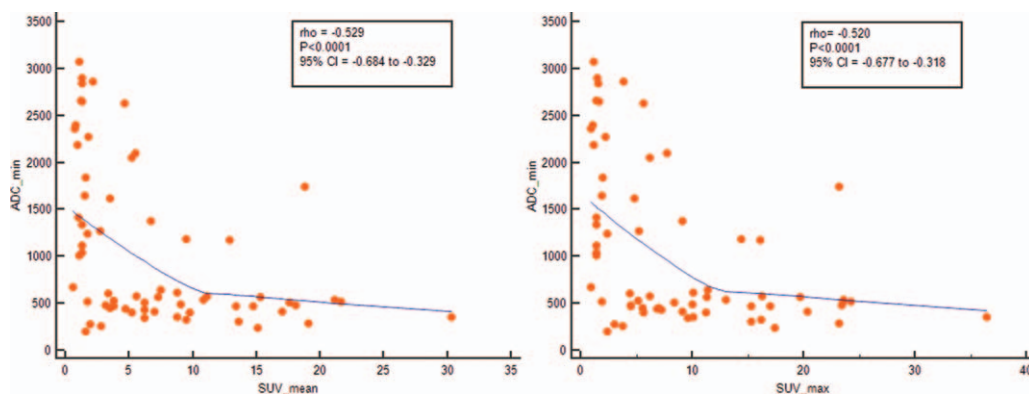


**Figure 4.** Scatter diagram with trend line showing correlation between ADCmin and SUVmean (left) and between ADCmean and SUVmax (right). ADCmean = mean ADC, SUVmean = mean SUV.

between ADCmin and SUVmean ( $\rho = -0.529, P < .0001$ ) and between ADCmin and SUVmax ( $\rho = -0.520, P < .0001$ ) (Table 3) (Fig. 4). ROC curve analysis showed AUC of 0.991, 0.992, 0.927 and 0.947 for SUVmax, SUVmean, ADCmin, and ADCmean, respectively (Table 4) (Figs. 5 and 6). The ROC curve of ADCmin versus SUVmax and SUVmean showed statistical significance (difference = 0.064,  $P = .038$  and difference = 0.065,  $P = .033$ ; respectively), but the ROC curve of ADCmean versus SUVmax and SUVmean was not statistically significant (difference = 0.044,  $P = .08$  and difference = 0.045,  $P = .07$ ; respectively). Interobserver variability of PET/MR metrics showed very good agreement for all variables (ADCmean [ICC = 0.95, 95% CI = 0.91–0.97], ADCmin [ICC = 0.87, 95% CI = 0.72–0.93], SUVmax [ICC = 0.99, 95% CI = 0.99–0.99], SUVmean [ICC = 0.98, 95% CI = 0.92–0.99]).

**4. Discussion**

The results of our study suggest a significant correlation between metabolic activity of glucose and cell density in nodal lymphoma lesions. It also show that quantitative MR ADCmean is almost equal to semiquantitative PET SUV measurements for discriminating positive from negative target nodal lymphoma in adult patients, with very good interobserver agreement.

PET/CT is presently the reference standard for evaluating patients with FDG-avid lymphoma.<sup>[4,10]</sup> Unfortunately, PET/CT involves exposure of lymphoma patients to a substantial dose of radiation that is repeatedly administered during follow-up and which may increase the risk of other malignancies, particularly in young patients with prolonged life expectancy.<sup>[1,14,19]</sup> Thus, there is a need for reducing the exposure to ionizing radiation in these patients. MR imaging provides very good tissue contrast resolution and is free of ionizing radiation.

Despite the adoption of visual analysis using D5PS and the Lugano Classification as the standard interpretation of PET, an objective reproducible quantifiable method is still needed to better determine not only the effectiveness of treatment but predict resistance to treatment and therefore improve the management of lymphoma patients.<sup>[4,10,23–26]</sup> In addition, quantitation is important both for sequential studies of single patients and for comparing different patient groups.<sup>[27]</sup> Semiquantitative assessment of FDG uptake has been reported with excellent sensitivity and specificity and very good interobserver reproducibility.<sup>[28]</sup> Lin et al,<sup>[29]</sup> compared visual analysis with SUVmax in lymphoma patients and showed that the semiquantitative measurements of FDG uptake were more accurate than visual analysis for predicting event-free survival. Itti et al,<sup>[30]</sup> also showed higher interobserver reproducibility and prognostic

**Table 4**  
Receiver operating characteristic (ROC) curve analysis.

Cutoff criterion	Receiver operating characteristic (ROC) curve analysis		
	Sensitivity (%) (95% CI)	Specificity (%) (95% CI)	Area under the curve (95% CI)
SUVmax >3.84	91.49 (79–97)	100 (82–100)	0.99 (0.93–1.0)
SUVmean >2.14	93.62 (82–100)	100 (82–100)	0.99 (0.93–1.0)
ADCmean ≤969	80.85 (67–91)	100 (82–100)	0.95 (0.86–0.98)
ADCmin ≤645	80.85 (67–91)	100 (82–100)	0.93 (0.83–0.97)

ADC = apparent diffusion coefficient (sec/mm<sup>2</sup>), ADCmean = mean ADC, ADCmin = minimal ADC, SUVmax = maximal SUV, SUVmean = mean SUV.

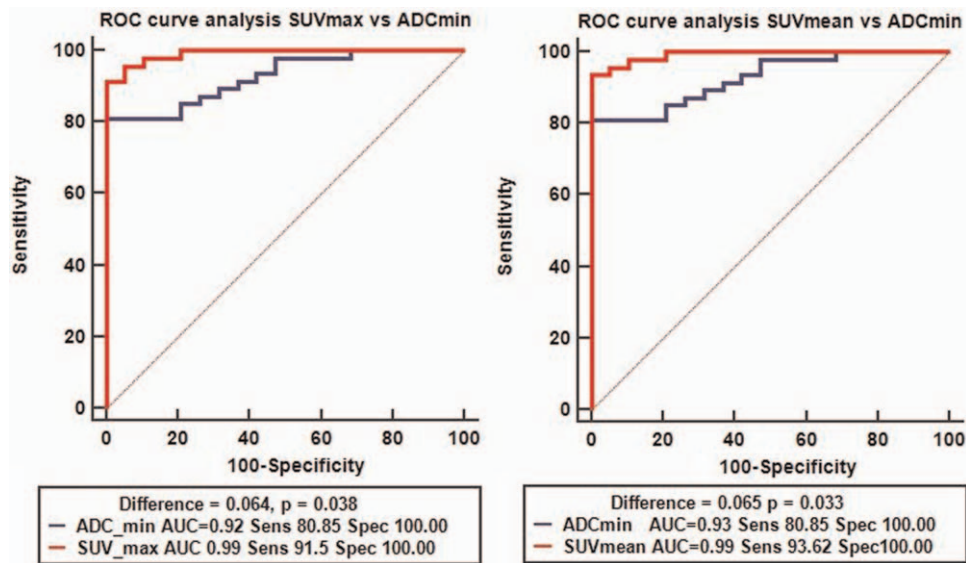


**Figure 5.** ROC curve analysis comparison between ADCmin and SUVs. ADCmean=mean ADC, ROC=receiver operating characteristic, SUV=standardized uptake value.

value of SUVmax compared to visual assessment. We found very good interobserver agreement of PET/MR semiquantitative PET SUVs and quantitative MR ADCs measurements.

The reported association between ADCs and SUVs in lymphoma patients has ranged from substantial to poor (from 0.65 to  $-0.64$ ).<sup>[1,11,31]</sup> We found a moderate inverse association between ADCmin and SUVs, and a substantial inverse association between ADCmean and SUVs. These results are expected since both methods measure different properties of tissues, rendering the association less definite.

On the other hand, our results showed that ADCmin and ADCmean were accurate for discriminating positive from negative nodal lymphoma, with an AUC of 0.927 and 0.947,

respectively. Although their sensitivity was slightly lower than that of SUVs, with a statistically significant difference in the accuracy between ADCmin and SUVs, there was no significant difference between the accuracy of SUVs and ADCmean. These results suggest that ADCmean may be the best quantitative MR DWI for assessment of nodal lymphomas.

Quantitation is inherent in PET and in MR imaging. The introduction of simultaneous PET/MR imaging offers a new modality that combines within a single imaging session high soft-tissue contrast resolution and cell density information of MR with metabolic imaging from PET. Therefore, the combined use of quantitative measurements from these imaging techniques could provide additional information to enhance the clinical

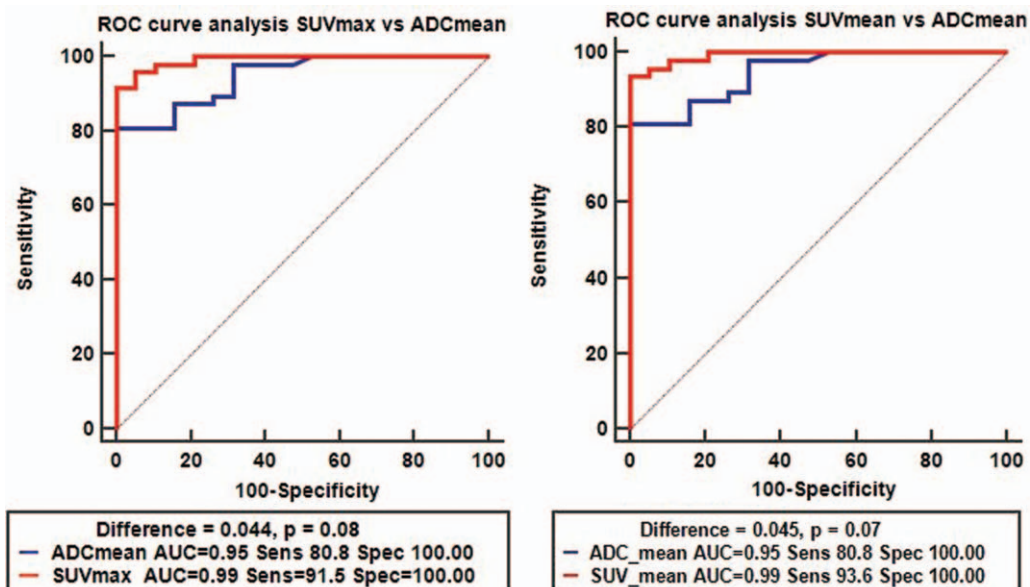


**Figure 6.** ROC curve analysis comparison between ADCmean and SUVs. ADCmean=mean ADC, ROC=receiver operating characteristic, SUV=standardized uptake value.

management of lymphoma patients. This modality has shown promising results in oncological imaging with very good reproducibility and repeatability of PET semiquantitative measurements and could be useful in the management of patients with FDG avid lymphoma and in FDG non-avid lymphoma.<sup>[26,27]</sup>

Our study has some limitations. First, this study was retrospective and the number of patients was limited, and therefore, its results should be confirmed in a larger study. Second, patients were selected from consecutive clinically-indicated PET/CT for lymphoma assessment thus, different types of lymphoma were included and the studies were not limited to baseline. Nonetheless, this heterogeneous population may provide supplementary information with previous and future radiomic studies regarding interobserver agreement and accuracy of quantitative measurements by FDG PET/MR and the future mining of this multiparametric data could be correlated with genomic and histopathological patterns to provide patients with precise medicine. Third, a single expert used all available FDG PET/CT and clinical information with a follow-up of at least 6 months to determine PET-positive and PET-negative nodal lymphoma. Although this information could have biased the detection of the regional positive lymphoma, the interobserver agreement for the D5PS has been shown to be high and an experienced and meticulous reader could detect PET-negative and -positive lymphoma that may have been difficult for others to duplicate. Fourth, the selection of only one limited PET/MR FOV based on baseline FDG PET/CT study may have prevented measurements of other local or regional lymph nodes that might have had different values; nevertheless the region with the most impressive FDG uptake region was selected, strongly suggesting lymphoma. Moreover, the main purpose of this study was specifically to compare quantitative PET/MR (SUVs and ADCs) and qualitative DWI visual assessment of nodal lymphoma; therefore, a short scanning time of less than 15 minutes was more reasonable and patients were more willing to participate. Fifth, as in several other studies, the reference standard was FDG PET/CT rather than histopathological sampling for each nodal lesion. However, FDG PET/CT is largely accepted as a reference standard in all baseline FDG-avid lymphoma histologies, including follicular lymphoma.<sup>[7,8]</sup>

In conclusion, a significant correlation between ADCs and SUVs is found in FDG avid lymphomas. ADCmean is not inferior to PET SUV in discriminating positive and negative nodal lymphomas. Further larger studies with a homogeneous population are warranted to validate quantitative PET/MR for lymphoma patient management.

### Author contributions

**Conceptualization:** Hanna Bernstine, Liran Domachevsky, Meital Nidam, Natalia Goldberg, Ifat Abadi-Korek, Ofer Shpilberg, David Groshar.

**Data curation:** Hanna Bernstine, Liran Domachevsky, Natalia Goldberg, Ofer Shpilberg, David Groshar.

**Formal analysis:** Hanna Bernstine, Liran Domachevsky, Meital Nidam, Natalia Goldberg, Ifat Abadi-Korek, Ofer Shpilberg, David Groshar.

**Investigation:** Liran Domachevsky, Ofer Shpilberg, David Groshar.

**Methodology:** Hanna Bernstine, Liran Domachevsky, Meital Nidam, Ifat Abadi-Korek, Ofer Shpilberg, David Groshar.

**Project administration:** David Groshar.

**Supervision:** David Groshar.

**Writing – original draft:** Hanna Bernstine, Liran Domachevsky, Meital Nidam, Ofer Shpilberg, David Groshar.

**Writing – review & editing:** Hanna Bernstine, Liran Domachevsky, Meital Nidam, Natalia Goldberg, Ifat Abadi-Korek, Ofer Shpilberg, David Groshar.

### References

- [1] Afaq A, Fraioli F, Sidhu H, et al. Comparison of PET/MRI with PET/CT in the evaluation of disease status in lymphoma. *Clin Nucl Med* 2017;42:e1–7.
- [2] Kirchner J, Deuschl C, Grueneisen J, et al. 18F-FDG PET/MRI in patients suffering from lymphoma: how much MRI information is really needed? *Eur J Nucl Med Mol Imaging* 2017;44:1005–13.
- [3] Atkinson W, Catana C, Abramson JS, et al. Hybrid FDG-PET/MR compared to FDG-PET/CT in adult lymphoma patients. *Abdom Radiol (NY)* 2016;41:1338–48.
- [4] Moghbel MC, Kostakoglu L, Zukotynski K, et al. Response assessment criteria and their applications in lymphoma: part 1. *J Nucl Med* 2016;57:928–35.
- [5] Dann EJ, Bairey O, Bar-Shalom R, et al. Modification of initial therapy in early and advanced Hodgkin lymphoma, based on interim PET/CT is beneficial: a prospective multicentre trial of 355 patients. *Br J Haematol* 2017;178:709–18.
- [6] Borchmann P, Haverkamp H, Lohri A, et al. Progression-free survival of early interim PET-positive patients with advanced stage Hodgkin's lymphoma treated with BEACOPP (escalated) alone or in combination with rituximab (HD18): an open-label, international, randomised phase 3 study by the German Hodgkin Study Group. *Lancet Oncol* 2017;18:454–63.
- [7] Cheson BD, Fisher RI, Barrington SF, et al. Recommendations for initial evaluation, staging, and response assessment of Hodgkin and non-Hodgkin lymphoma: the Lugano classification. *J Clin Oncol* 2014;32:3059–68.
- [8] Ladetto M, Buske C, Hutchings M, et al. ESMO consensus conference on malignant lymphoma: general perspectives and recommendations for prognostic tools in mature B-cell lymphomas and chronic lymphocytic leukaemia. *Ann Oncol* 2016;27:2149–60.
- [9] Younes A, Hilden P, Coiffier B, et al. International Working Group consensus response evaluation criteria in lymphoma (RECIL 2017). *Ann Oncol* 2017;28:1436–47.
- [10] Moghbel MC, Mittra E, Gallamini A, et al. Response assessment criteria and their applications in lymphoma: part 2. *J Nucl Med* 2017;58:13–22.
- [11] Deng S, Wu Z, Wu Y, et al. Meta-analysis of the correlation between apparent diffusion coefficient and standardized uptake value in malignant disease. *Contrast Media Mol Imaging* 2017;2017:4729547.
- [12] Barrington SF, Mikhael NG, Kostakoglu L, et al. Role of imaging in the staging and response assessment of lymphoma: consensus of the International Conference on Malignant Lymphomas Imaging Working Group. *J Clin Oncol* 2014;32:3048–58.
- [13] Albano D, Patti C, La Grutta L, et al. Comparison between whole-body MRI with diffusion-weighted imaging and PET/CT in staging newly diagnosed FDG-avid lymphomas. *Eur J Radiol* 2016;85:313–8.
- [14] Balbo-Mussetto A, Cirillo S, Bruna R, et al. Whole-body MRI with diffusion-weighted imaging: a valuable alternative to contrast-enhanced CT for initial staging of aggressive lymphoma. *Clin Radiol* 2016;71:271–9.
- [15] Littooj AS, Kwee TC, de Keizer B, et al. Whole-body MRI-DWI for assessment of residual disease after completion of therapy in lymphoma: a prospective multicenter study. *J Magn Reson Imaging* 2015;42:1646–55.
- [16] Mayerhoefer ME, Karanikas G, Kletter K, et al. Evaluation of diffusion-weighted magnetic resonance imaging for follow-up and treatment response assessment of lymphoma: results of an 18F-FDG-PET/CT-controlled prospective study in 64 patients. *Clin Cancer Res* 2015;21:2506–13.
- [17] Tsuji K, Kishi S, Tsuchida T, et al. Evaluation of staging and early response to chemotherapy with whole-body diffusion-weighted MRI in malignant lymphoma patients: a comparison with FDG-PET/CT. *J Magn Reson Imaging* 2015;41:1601–7.
- [18] Taouli B, Koh DM. Diffusion-weighted MR imaging of the liver. *Radiology* 2010;254:47–66.
- [19] Hagtvædt T, Seierstad T, Lund KV, et al. Diffusion-weighted MRI compared to FDG PET/CT for assessment of early treatment response in lymphoma. *Acta Radiol* 2015;56:152–8.

- [20] Herrmann K, Queiroz M, Huellner MW, et al. Diagnostic performance of FDG-PET/MRI and WB-DW-MRI in the evaluation of lymphoma: a prospective comparison to standard FDG-PET/CT. *BMC Cancer* 2015;15:1002.
- [21] van Ufford HM, Kwee TC, Beek FJ, et al. Newly diagnosed lymphoma: initial results with whole-body T1-weighted, STIR, and diffusion-weighted MRI compared with 18F-FDG PET/CT. *AJR Am J Roentgenol* 2011;196:662–9.
- [22] Cheson BD, Ansell S, Schwartz L, et al. Refinement of the Lugano classification lymphoma response criteria in the era of immunomodulatory therapy. *Blood* 2016;128:2489–96.
- [23] Ferdova E, Ferda J, Baxa J. 18F-FDG-PET/MRI in lymphoma patients. *Eur J Radiol* 2017;94:A52–63.
- [24] Barrington SF, Kluge R. FDG PET for therapy monitoring in Hodgkin and non-Hodgkin lymphomas. *Eur J Nucl Med Mol Imaging* 2017;44:97–110.
- [25] Derclé L, Seban RD, Lazarovici J, et al. 18F-FDG PET and CT-scan detect new imaging patterns of response and progression in patients with Hodgkin lymphoma treated by anti-PD1 immune checkpoint inhibitor. *J Nucl Med* 2017;59:15–24.
- [26] Law WP, Maggacis N, Jeavons SJ, et al. Concordance of 18F-FDG PET uptake in tumor and normal tissues on PET/MRI and PET/CT. *Clin Nucl Med* 2017;42:180–6.
- [27] Groshar D, Bernstine H, Goldberg N, et al. Reproducibility and repeatability of same-day two sequential FDG PET/MR and PET/CT. *Cancer Imaging* 2017;17:11.
- [28] Han EJ, O JH, Yoon H, et al. FDG PET/CT response in diffuse large B-cell lymphoma: reader variability and association with clinical outcome. *Medicine (Baltimore)* 2016;95:e4983.
- [29] Lin C, Itti E, Haioun C, et al. Early 18F-FDG PET for prediction of prognosis in patients with diffuse large B-cell lymphoma: SUV-based assessment versus visual analysis. *J Nucl Med* 2007;48:1626–32.
- [30] Itti E, Lin C, Dupuis J, et al. Prognostic value of interim 18F-FDG PET in patients with diffuse large B-Cell lymphoma: SUV-based assessment at 4 cycles of chemotherapy. *J Nucl Med* 2009;50:527–33.
- [31] Giraudo C, Raderer M, Karanikas G, et al. 18F-Fluorodeoxyglucose positron emission tomography/magnetic resonance in lymphoma: comparison with 18F-fluorodeoxyglucose positron emission tomography/computed tomography and with the addition of magnetic resonance diffusion-weighted imaging. *Invest Radiol* 2016;51:163–9.